Scaling ansatz for the jamming transition

Carl P. Goodrich[a,b,1], Andrea J. Liu[a], and James P. Sethna[c]

[a]Department of Physics, University of Pennsylvania, Philadelphia, PA 19104; [b]School of Engineering and Applied Sciences, Harvard University, Cambridge, MA 02138; and [c]Department of Physics, Cornell University, Ithaca, NY 14850

Edited by Sharon C. Glotzer, University of Michigan, Ann Arbor, MI, and approved June 29, 2016 (received for review February 2, 2016)

We propose a Widom-like scaling ansatz for the critical jamming transition. Our ansatz for the elastic energy shows that the scaling of the energy, compressive strain, shear strain, system size, pressure, shear stress, bulk modulus, and shear modulus are all related to each other via scaling relations, with only three independent scaling exponents. We extract the values of these exponents from already known numerical or theoretical results, and we numerically verify the resulting predictions of the scaling theory for the energy and residual shear stress. We also derive a scaling relation between pressure and residual shear stress that yields insight into why the shear and bulk moduli scale differently. Our theory shows that the jamming transition exhibits an emergent scale invariance, setting the stage for the potential development of a renormalization group theory for jamming.

jamming transition | scaling ansatz | nonequilibrium critical phenomena

The existence of criticality at the jamming transition suggests that universal physics underlies rigidity in disordered solids ranging from glasses to granular materials (1). The jamming transition marks the onset of rigidity in athermal sphere packings and was originally proposed as a zero-temperature transition (2, 3) for soft repulsive spheres in a nonequilibrium "jamming phase diagram" (4) of varying packing density and applied shear. Many studies have documented behaviors characteristic of critical phenomena near the jamming transition, including power law scaling (2, 3, 5) and scaling collapses (6–13) of numerous properties, with the expression of quantities in terms of scaling functions, diverging length scales (6, 14–19), and finite-size scaling (10, 12, 20). Theories have been developed to individually understand and relate some of these power laws (15, 16, 21, 22), but a unified scaling theory has been lacking. Here, we develop such a theory by proposing a scaling ansatz for the jamming critical point in terms of the fields originally identified by the jamming phase diagram, namely density and shear.

The critical point scaling ansatz introduced by Widom (23) in the 1960s was a key advance in the theory of critical phenomena that set the stage for the development of the renormalization group. The ansatz writes the state functions near continuous equilibrium phase transitions in terms of power law ratios of the control parameters. By positing a scaling function for the free energy, it exploits the fact that quantities, such as the specific heat, magnetization, and susceptibility, are derivatives of the free energy to derive relations not only among their scaling exponents but among their scaling functions. Thus, the scaling ansatz provides a unified and comprehensive description of systems exhibiting what later was realized to be an emergent scale invariance.

Unlike most systems exhibiting a dynamical scale invariance, we find that a jammed system can also be viewed as a material with critical properties that are determined by a state function, analogous to those at thermodynamic critical points. We introduce a scaling ansatz for the elastic energy of a sphere packing just above the jamming transition to develop a unified theory of the scaling exponents and scaling functions for the energy, excess packing fraction, shear strain, pressure, shear stress, bulk modulus, shear modulus, and system size. Our theory yields scaling relations that relate the singular behavior of all of these quantities to only three independent scaling exponents, which can be extracted from known numerical and theoretical results. It predicts exponents for the shear stress and shear strain. Most importantly, however, our scaling theory shows how the jamming transition can be understood in the context of the theory of critical phenomena.

Scaling Ansatz

We consider d-dimensional jammed packings of soft frictionless spheres at temperature $T=0$ with packing fraction ϕ (details are in *Materials and Methods*). Note that the packing fraction at the jamming transition, $\phi_{c,\Lambda}$, varies from one member of the ensemble, Λ, to the next. For each packing, we characterize the distance above the transition by $\Delta\phi \equiv \phi - \phi_{c,\Lambda}$.* Systems are further characterized by the average number of interacting neighbors per particle (the contact number Z), which satisfies $Z \geq Z_{\min}$ where $Z_{\min} = 2d - (2d-2)/N$ approaches the isostatic value $Z_{\text{iso}} \equiv 2d$ in the thermodynamic limit (3, 10). A key quantity used extensively in this paper is the excess contact number (the number of contacts per particle in excess of the minimum value), namely $\Delta Z = Z - Z_{\min}$. For a given protocol for preparing jammed states, the mean dimensionless (*Materials and Methods*) energy density E of a sphere packing will depend on ΔZ and $\Delta\phi$ as well as the shear strain ε and the system size N. We define ε relative to the strain of the as-quenched state.

Significance

Central to the theory of phase transitions is the fact that the free energy can be written in a scale-invariant form that captures scaling exponent relations. Our work shows that, for the jamming transition, the elastic energy is the relevant free energy and can be expressed in a scale-invariant form consistent with known exponent relations. This result places jamming in the context of the theory of critical phenomena, suggesting the potential for a theoretical description of jamming on par with that of Ising criticality. It also provides powerful support for the idea that the observed commonality in the mechanical and thermal responses of disordered solids can be understood as a manifestation of universality associated with the critical jamming transition.

Author contributions: C.P.G., A.J.L., and J.P.S. designed research, performed research, analyzed data, and wrote the paper.

The authors declare no conflict of interest.

This article is a PNAS Direct Submission.

Freely available online through the PNAS open access option.

See Commentary on page 9673.

[1]To whom correspondence should be addressed. Email: goodrich@g.harvard.edu.

This article contains supporting information online at www.pnas.org/lookup/suppl/doi:10.1073/pnas.1601858113/-/DCSupplemental.

*This configuration-dependent critical density is similar to many other systems with sharp global transitions in behavior as originally discovered in the depinning of charge–density waves (24–26). Such systems may not obey the inequality between the correlation length and dimension $\nu \geq 2/d$ derived for equilibrium systems, unless analyzed using deviations from the infinite system critical point (27). In jamming, not only does the critical density fluctuate because of finite-size effects, it is also known that, even in the thermodynamic limit, the critical density depends on the protocol (20, 28). However, the dependence of quantities, such as those discussed here, on the distance above each system's critical density seems to be insensitive to protocol (28). Here, we use the system-dependent critical density as suggested in refs. 2 and 3, which allows closer scrutiny of scaling near the jamming transition.

We first present the scaling ansatz and then show that it agrees with known scalings and correctly predicts the scaling exponent for the shear stress. Our scaling ansatz is

$$E(\Delta Z, \Delta\phi, \varepsilon, N) = \Delta Z^{\zeta}\mathcal{E}_0\left(\frac{\Delta\phi}{\Delta Z^{\beta_\phi}}, \frac{\varepsilon}{\Delta Z^{\beta_\varepsilon}}, N\Delta Z^{\psi}\right), \quad [1]$$

where the scaling exponents ζ, β_ϕ, β_ε and ψ are yet to be determined. Eq. **1** is set up so that the leading singular part of the elastic energy in the thermodynamic limit is proportional to ΔZ^{ζ}. The excess packing fraction $\Delta\phi$ and shear strain ε represent components of the same strain tensor (compression and shear, respectively) but are allowed to scale differently.[†] Allowing $\Delta\phi$ and ε to scale differently would seem natural, because they are different "relevant directions" in the jamming phase diagram. The different exponents lead to different scaling properties for the bulk and shear moduli B and G, respectively.[‡]

Jamming is believed to have an upper critical dimension of $d_u = 2$ (1, 10, 21, 30–33). There is close agreement between the numerical exponent for the shear modulus in dimensions $d = 2,3$ (3, 5, 10) with the analytical result of $G \sim \Delta Z^1$ in $d = \infty$ (34). More compellingly, the use of the total number of particles, $N \sim L^d$, rather than the more traditional system length L to characterize system size in the finite-size scaling collapse allows the critical exponent for the shear modulus to be independent of dimension for $d = 2,3$ (10). This fact provides strong evidence that $d_u = 2$, because finite-size effects should scale with $N \sim L^d$ (35, 36) instead of L for $d \geq d_u$. This reasoning underlies our choice of the form of the last argument of the function $\mathcal{E}_0$ in Eq. **1**. It also justifies our use of integer and half-integer values for the various critical exponents in the analyses that follow (34).

Finally, note that, for a given preparation protocol, jammed packings at a given $\Delta\phi$, N, and ε have a prescribed average value of ΔZ, so that ΔZ is not a variable that can be tuned independently. Until now, it has not been clear whether the natural control variable for the problem (analogous to reduced temperature in the Ising model) should be ΔZ, $\Delta\phi$, or p. We find that corrections to scaling suggest that ΔZ should be the natural control variable (*SI Text*); in addition, the formulation is more elegant if we treat ΔZ as an independent variable, so that the form of Eq. **1** is the same with respect to compressive strain and shear strain. The use of ΔZ as an independent variable is somewhat analogous to the use of a variable magnetization in Landau theory of magnets, where the free energy density at fixed external field and temperature is expressed as a function of magnetization, although the equilibrium magnetization is set by the field and temperature.

We proceed by calculating derivatives of the energy (Eq. **1**) with respect to $\Delta\phi$ and ε to obtain scaling expressions for the pressure p and the residual shear stress s:

$$p \equiv \phi\frac{dE}{d\Delta\phi} = \Delta Z^{\delta_p}\mathcal{P}_0\left(\frac{\Delta\phi}{\Delta Z^{\beta_\phi}}, \frac{\varepsilon}{\Delta Z^{\beta_\varepsilon}}, N\Delta Z^{\psi}\right) \quad [2]$$

and

$$s \equiv \frac{dE}{d\varepsilon} = \Delta Z^{\delta_s}\mathcal{S}_0\left(\frac{\Delta\phi}{\Delta Z^{\beta_\phi}}, \frac{\varepsilon}{\Delta Z^{\beta_\varepsilon}}, N\Delta Z^{\psi}\right). \quad [3]$$

Similarly, the bulk modulus B and shear modulus G are second derivatives of the energy, taking the forms

$$B \equiv \frac{\phi^2}{2}\frac{d^2E}{d\Delta\phi^2} = \Delta Z^{\gamma_B}\mathcal{B}_0\left(\frac{\Delta\phi}{\Delta Z^{\beta_\phi}}, \frac{\varepsilon}{\Delta Z^{\beta_\varepsilon}}, N\Delta Z^{\psi}\right) \quad [4]$$

and

$$G \equiv \frac{d^2E}{d\varepsilon^2} = \Delta Z^{\gamma_G}\mathcal{G}_0\left(\frac{\Delta\phi}{\Delta Z^{\beta_\phi}}, \frac{\varepsilon}{\Delta Z^{\beta_\varepsilon}}, N\Delta Z^{\psi}\right). \quad [5]$$

Note that the factors of ϕ and ϕ^2 that appear in Eqs. **2** and **4** are slowly varying and can be treated as constant near the singularity. Also, note that the scaling functions $\mathcal{P}_0$, $\mathcal{S}_0$, $\mathcal{B}_0$, and $\mathcal{G}_0$ can be written explicitly as functions of $\mathcal{E}_0$ and its derivatives.

Eqs. **2**–**5** are constructed for a "fixed $\Delta\phi\varepsilon N$" ensemble and show that the pressure and shear stress arise naturally for this ensemble as order parameters that scale with powers of the excess contact number, ΔZ. In this ensemble, p and s are analogous to the magnetization, whereas $\Delta\phi$ and ε are analogous to the magnetic field in the Ising model. However, it is straightforward to use Legendre transformations to convert to other ensembles, such as the "fixed $p\varepsilon N$" ensemble that is common in the numerical literature (*SI Text*) or the "fixed psN" ensemble of ref. 9. We emphasize that the scaling of all variables with ΔZ is not affected by the ensemble in which one works. However, in the fixed psN ensemble, $\Delta\phi$ and ε are order parameters, whereas p and s play the role of the magnetic field in the Ising model. The latter ensemble leads to second derivatives B^{-1} and G^{-1}, where G^{-1} diverges at the transition, in more direct analogy to the magnetic susceptibility as the diverging second derivative of the free energy with respect to magnetic field in the Ising model. Our notation for the exponents β_ϕ, β_ε, δ_p, δ_s, γ_B, and γ_G therefore conforms to the scaling theory natural for the fixed psN ensemble.

The scaling forms of Eqs. **2**–**5** imply four exponent relations:

$$\begin{aligned} \delta_p &= \zeta - \beta_\phi, \\ \delta_s &= \zeta - \beta_\varepsilon, \\ \gamma_B &= \zeta - 2\beta_\phi, \\ \text{and } \gamma_G &= \zeta - 2\beta_\varepsilon. \end{aligned} \quad [6]$$

We will later derive an additional exponent relation, $\delta_s = \delta_p + \psi/2$. Eqs. **1**–**5** contain eight exponents, and therefore, the entire theory is expressed in terms of only three independent scaling exponents.

Extracting Exponents and Numerical Verification

We now use known scaling laws to extract numerical values for the exponents in our theory.

SI Text shows how to manipulate Eqs. **1**–**5** to directly compare with numerical simulations. The manipulation is straightforward and involves converting to the fixed $p\varepsilon N$ ensemble (which has become standard in the numerical literature for jamming), integrating over the ΔZ distribution, and explicitly setting the shear strain to zero. This process results in the following scaling predictions from the ansatz:

$$E = \Delta Z^{\zeta}\mathcal{E}(N\Delta Z^{\psi}), \quad [7]$$

$$\Delta\phi = \Delta Z^{\beta_\phi}\Phi(N\Delta Z^{\psi}), \quad [8]$$

$$s = \Delta Z^{\delta_s}\mathcal{S}(N\Delta Z^{\psi}), \quad [9]$$

[†]Different shear directions are statistically equivalent, because systems are prepared isotropically, and therefore, we represent them with a single ε.

[‡]Clearly, bulk and shear moduli need not scale together—liquids form a counterexample. At the critical jamming transition separating a nonequilibrium jammed solid from a repulsive gas of nonoverlapping spheres, the bulk and shear moduli share features of a liquid ($G = 0$ and $B > 0$). This behavior is reminiscent of the metal-like resistivity at the 2D disordered critical point separating superconductors and insulators (29).

$$B = \Delta Z^{\gamma_B} \mathcal{B}(N\Delta Z^{\psi}), \quad [10]$$

and

$$G = \Delta Z^{\gamma_G} \mathcal{G}(N\Delta Z^{\psi}) \quad [11]$$

as well as

$$N^{\frac{1}{\psi}}\Delta Z = \mathcal{Z}\left(Np^{\frac{\psi}{\delta_p}}\right). \quad [12]$$

Note that B, G, and ΔZ should become independent of N in the large N limit, and it is well-established that $\Delta Z \sim p^{1/2}$, $B \sim \Delta Z^0$ and $G \sim \Delta Z$ in this regime (3, 5, 12). Furthermore, recent studies of finite-size effects found that $N\Delta Z = F(Np^{1/2})$ (10, 12).[§] Comparing these results with Eqs. **10**–**12**, we see that $\delta_p = 2$, $\gamma_B = 0$, $\gamma_G = 1$ and $\psi = 1$. Using the exponent equalities of Eq. **6**, we also find $\zeta = 4$, $\beta_\phi = 2$, $\beta_\varepsilon = 3/2$ and $\delta_s = 5/2$. These exponents are summarized in Table 1.

Note that the scaling exponents can be obtained alternatively by appealing to theoretical arguments for the scaling of the shear modulus, contact number, and length scale (21), leading to a completely theoretical derivation of the exponents and scaling relations (*SI Text*).

Our scaling theory yields predictions for the scaling of E, $\Delta\phi$, and s in Eqs. **7**–**9**. To test these predictions numerically, we generate jammed sphere packings in the fixed $p\varepsilon N$ ensemble, which is described in *Materials and Methods*. We first consider the energy density E, which is shown as a function of ΔZ in Fig. 1*A* for systems in three dimensions ($d = 3$). The clear finite-size effects collapse quite well when the data are scaled according to Eq. **7** with $\zeta = 4$ and $\psi = 1$ (Fig. 1*B*) as predicted.

We now turn to the scaling of the shear stress s. Our packings are prepared isotropically at $\varepsilon = 0$, and therefore, the residual stress fluctuates around zero. We, therefore, consider the average of $s^2 \equiv \mathrm{Tr}\left[\sigma - \frac{1}{d}\mathrm{Tr}\,\sigma\right]^2$, where σ is the stress tensor. This average is shown as a function of ΔZ in Fig. 2*A*. To collapse these data, we note that s^2 vanishes in the infinite system size limit as $1/N$ (*Pressure–Shear Stress Exponent Equality*), consistent with the central limit theorem. It is, therefore, convenient to factor out one power of $(N\Delta Z^{\psi})^{-1}$ from the scaling function for s^2 analogous to Eq. **9**:

$$s^2 = \Delta Z^{2\delta_s}\left[(N\Delta Z^{\psi})^{-1}\mathcal{S}_2(N\Delta Z^{\psi})\right]. \quad [13]$$

This predicted scaling collapse is verified numerically in Fig. 2*B* with $\delta_s = 5/2$ and $\psi = 1$. Finally, as expected from classical scaling theories, Fig. 2*C* shows that our theory also describes the distributions of quantities: in this case, s^2.

The *SI Text* shows data for the energy, pressure, shear stress, bulk modulus, and shear modulus in 2D (Fig. S1) and 3D (Fig. S2). The scaling collapses for 3D systems are even more successful if one includes analytic corrections to scaling (Fig. S3). The collapses for 2D systems are reasonable but not quite as successful, likely because of corrections to scaling expected in the upper critical dimension as observed previously (12, 13); however, they are otherwise consistent with our theory with the same exponents as in $d = 3$.

Finally, note that Eqs. **2** and **3** are stress–strain relations, and the well-known compressional stress relation $p \sim \Delta\phi$ (3, 5) emerges from the scaling ansatz. Similarly, the scaling collapse of the shear stress–strain relation, obtained by integrating Eq. **S5** as in *SI Text*, so that $s = \Delta Z^{\delta_s}\mathcal{S}_\infty(\varepsilon/\Delta Z^{\beta_\varepsilon}, N\Delta Z^{\psi})$, is consistent with that obtained earlier for harmonic spring networks (37). The scaling ansatz also yields a prediction for the scaling of the excess contact number $\Delta Z \sim \varepsilon^{1/\beta_\varepsilon}$ with strain ε at the jamming transition and the dependence of various quantities on s (e.g., figure 10 of ref. 12) when s is controlled as in the fixed psN ensemble (9). The scaling of s with ε and p predicted by the scaling theory has already been tested in recent numerical calculations (38, 39).

[§]Note that the finite-size analyses in refs. 10 and 12 also found that $GN = F_G(Np^{1/2})$, which is consistent with Eq. **11** and the exponents in Table 1, thus providing the first check of our scaling theory.

Table 1. List of scaling exponents and their approximate values

	Exponent							
	ζ	β_ϕ	β_ε	ψ	δ_p	δ_s	γ_B	γ_G
Value	4	2	3/2	1	2	5/2	0	1

As discussed in the text, numerical studies suggest that jamming exponents are close to integer or half-integer values, as presented here. These eight exponents are related by five exponent relations (Eqs. **6** and **16**), leaving three independent critical exponents.

Discussion

Many nonequilibrium phenomena exhibit power laws and are described by scaling functions; however, they cannot be framed in the context of the theory of equilibrium critical phenomena, because they cannot be described in terms of state functions. The jamming transition is at zero temperature, deep below the dynamical glass transition, and its behavior depends on how the system was prepared. It has long been recognized that jammed systems obey clean scaling behaviors when considered relative to the configuration-dependent critical packing fraction $\phi_{c,\Lambda}$ (3, 28). What our work shows is that all of the nonequilibrium aspects of the properties studied here are captured in $\phi_{c,\Lambda}$, so that after we choose to describe behavior in terms of $\Delta\phi = \phi - \phi_{c,\Lambda}$, the system can be described as a material in terms of a state function, namely the elastic energy. Thus, jamming provides a rare example of a nonequilibrium transition that can be understood, at least partially, within the framework of equilibrium critical phenomena.

The facts that the mean stress (unlike the pressure) remains zero for systems above the jamming transition and that the variance of the stress fluctuations scales as $1/N$ shed light on why the bulk modulus scales differently from the shear modulus at the jamming transition. In *Pressure–Shear Stress Exponent Equality*, we analyze the pressure and stress fluctuations microscopically and derive an important exponent relation, $2\delta_s - \psi = 2\delta_p$ (Eq. **16**), between the singularities of stress and pressure, which also yields the relation $\gamma_G = \gamma_B + \psi$ between the shear and bulk moduli. This

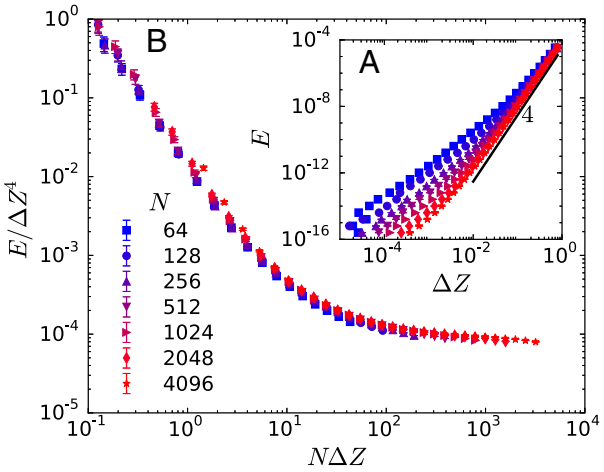

Fig. 1. Scaling collapse of the energy. (*A*) Energy as a function of ΔZ. (*B*) Energy scaled according to Eq. **1** using the predicted exponents $\zeta = 4$ and $\psi = 1$.

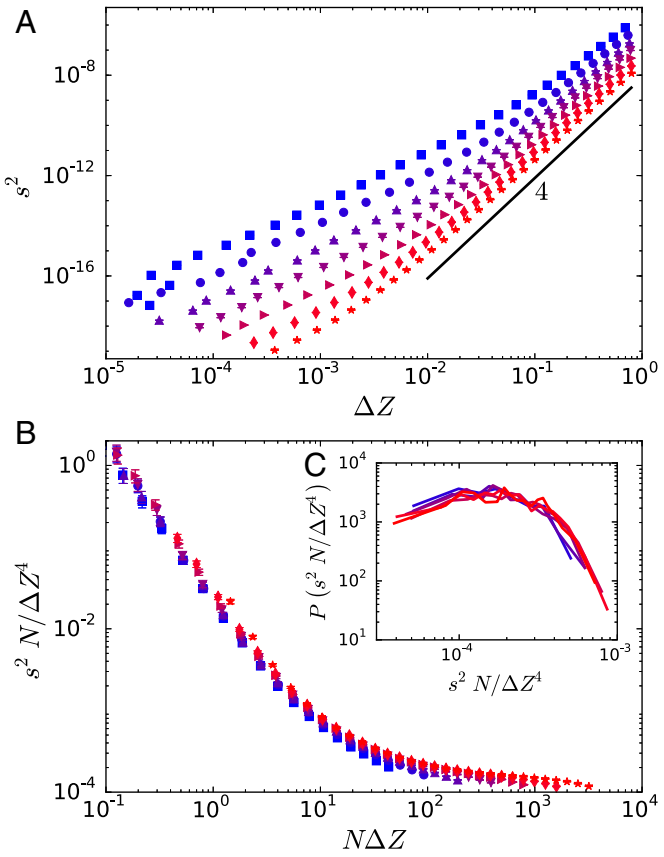

Fig. 2. Scaling collapse of the residual shear stress: (*A*) s^2 as a function of ΔZ, (*B*) s^2 scaled according to Eq. **13** using the predicted exponents $\delta_s = 5/2$ and $\psi = 1$, and (*C*) probability distribution of $s^2 N/\Delta Z^4$ for systems at fixed $N\Delta Z$ ($50 \le N\Delta Z \le 52$) and fixed $p/\Delta Z^2$ ($7.9\times10^{-3} \le p/\Delta Z^2 \le 8.3\times10^{-3}$). For $N = 64$, insufficient data exist in these ranges to calculate a distribution. Symbols and colors have the same meanings as in Fig. 1.

analysis uses the lack of long-range bond orientational order to derive the exponent relation; hence, we expect that shear-jammed systems (40) will have some components of their shear modulus that scale as the bulk modulus as jamming is approached (because shear jamming will yield long-ranged bond orientation correlations), which was also predicted in ref. 41.

Just as for equilibrium critical points, the dynamics of jamming at frequency ω is controlled by an additional invariant scaling combination $\omega/\Delta Z^{\delta_\omega}$, which is not part of the free energy and depends on what properties are conserved by the dynamics. Tighe (42) studied the complex shear modulus $G(\omega)$ and showed, for overdamped dynamics, that $G(\omega) = \Delta Z^{\gamma_G} \mathcal{G}(\omega/\Delta Z^{\delta_\omega})$, with $\delta_\omega \approx 2$. For undamped dynamics (15, 42), $\delta_\omega = 1$ (for example, controlling the cross-over frequency ω^* in both longitudinal and transverse phonons to the boson peak due to jamming) (14, 15). Since the longitudinal and transverse speeds of sound $c_L \sim \sqrt{B/\rho}$ and $c_T \sim \sqrt{G/\rho}$ scale differently near jamming, the longitudinal cross-over wavelength is $\ell_L \sim c_L/\omega^* \sim \Delta Z^{\gamma_B/2-\delta_\omega} \sim \Delta Z^{-1}$, whereas the transverse cross-over wavelength is $\ell_T \sim c_T/\omega^* \sim \Delta Z^{\gamma_G/2-\delta_\omega} \sim \Delta Z^{-1/2}$ (14). Note that, in $d = 2$ (the upper critical dimension), we can convert $N \sim L^2$ to rewrite the argument $N\Delta Z^\psi$ in Eq. **1** as $L\Delta Z^\nu$, where ν is a correlation length exponent. We see that the resulting length scale, $\xi \sim \Delta Z^{-\nu}$, has $\nu = \psi/2 = 1/2$, which has the same scaling as ℓ_T (14, 18). Interestingly, ref. 43 recently showed that finite-size effects governing flow in non-Brownian suspensions below the jamming transition scale as $N(Z_{\rm iso} - Z)^\Psi$, with ψ also equal to one. It remains to be seen if and how ℓ_L, which is also understood as the rigidity length ℓ^* that controls the excess low-frequency vibrational modes (15, 17), enters into the scaling theory.

In standard scaling theories, one expects the free energy density to scale as T/ξ^d from dimensional analysis for dimensions at or below the upper critical dimension (hyperscaling). Eq. **1** would then imply that $\Delta Z^\zeta = \Delta Z^{d\nu}$, so that $\zeta = d\nu$. In our case, $\nu = 1/2$ in $d = 2$ and $\zeta = 4$, violating hyperscaling, presumably because the jamming transition is at $T = 0$. A similar situation arises for the random field Ising model (44).

To extend to nonzero temperatures near the jamming transition, it is best to convert to the fixed *psN* ensemble, because strains become problematic in systems that can undergo rearrangement events. In that case, the scaling ansatz for the free energy becomes

$$F(\Delta Z, p, s, N, T) = \Delta Z^\zeta \mathcal{F}_0\left(\frac{p}{\Delta Z^{\delta_p}}, \frac{s}{\Delta Z^{\delta_s}}, N\Delta Z^\psi, \frac{T}{\Delta Z^{\delta_T}}\right). \quad [14]$$

If one then argues that, at high T, the free energy should not vanish or diverge at $\Delta Z = 0$ and should scale as T, one obtains $\delta_T = \zeta = 4$, consistent with the scaling of the cross-over temperature $T^* \sim \Delta Z^4$ governing whether the system obeys jamming behavior ($T < T^*$) or glassy behavior ($T > T^*$) (45, 46). However, for $T > 0$, issues, such as timescales and aging, become important, and we will leave a more thorough exploration for future work. For the same reason, we have not yet generalized the theory to thermal hard spheres at densities below the jamming transition, where similar power law scaling and diverging length scales arise (16, 47, 48), or to nonlinear responses necessary for describing avalanches (49) and shear flow (50).

In summary, we have proposed a Widom-like scaling ansatz for the jamming transition that ties together the behavior of thermodynamic quantities at densities above the jamming transition. It contains three independent exponents and predicts two nontrivial exponents. One of these exponents (δ_s) we have verified here using numerical simulations, and the other (β_ε) has been the subject of recent research (38, 39). The fact that the jamming transition can be described by a scaling ansatz implies that the jamming transition exhibits emergent scale invariance and that the tools of the theory of equilibrium critical phenomena, such as coarse graining and rescaling to study renormalization group flows, should be applicable. The scaling ansatz is, therefore, an important step toward a complete theoretical description of the jamming transition capable of systematically including friction, nonspherically symmetric potentials, three-body interactions, and other features of the real world to understand the extent of universality in the mechanical properties of disordered solids.

Materials and Methods

Definition of Jammed Sphere Packing. We consider disordered systems of N soft frictionless spheres in a d-dimensional periodic box of volume V. Systems are at temperature $T = 0$ and thus sit in a local minimum of the energy landscape defined by the pairwise interaction potential

$$U(r_{ij}) = \frac{U_0}{\alpha}\left(1 - \frac{r_{ij}}{R_i + R_j}\right)^\alpha \Theta\left(1 - \frac{r_{ij}}{R_i + R_j}\right), \quad [15]$$

where r_{ij} is the distance between the centers of particles i and j, R_i and R_j are the particles' radii, $\Theta(x)$ is the Heaviside step function, and U_0 sets the energy scale. The packing fraction is $\phi = V^{-1}\sum_i V_i$, where V_i is the d-dimensional volume of particle i, and the shear strain ε is defined relative to the strain of the as-quenched state. We define an effective spring constant, $k_{\rm eff} = U_0(\alpha-1)D_{\rm avg}^{-2}\Delta Z^{2(\alpha-2)}$ (51), where $D_{\rm avg}$ is the average particle diameter. We then rescale energy, pressure, shear stress, bulk modulus, and shear modulus by $k_{\rm eff}$ with appropriate factors of $D_{\rm avg}$, so that $E = {\rm energy}/k_{\rm eff}D_{\rm avg}^2$, $p = {\rm pressure}\times D_{\rm avg}/k_{\rm eff}$, and so on. The scaling ansatz presented in Eq. **1** is for these scaled quantities and does not depend on the exponent α in Eq. **15**.

Numerical Generation of Jammed Sphere Packings. We generate jammed sphere packings in the fixed $p\varepsilon N$ ensemble as follows. Particles are initially placed at random in a square or cubic periodic box at a very large packing fraction. We then quench the system to a local energy minimum corresponding to a

zero-temperature configuration using the FIRE algorithm (52). We then systematically adjust the packing fraction until we reach a target pressure (to within 1% accuracy). Starting from this final configuration, we repeat this process with a slightly lower target pressure. By continuously lowering the target pressure, we produce mechanically stable packings over a range of pressures (between $p = 10^{-8}$ and $p = 10^{-1}$) and system sizes (between $N = 64$ to $N = 4{,}096$) with $\varepsilon = 0$. Approximately 5,000 configurations are generated for each combination of p and N. We focus in the text on $d = 3$ systems with harmonic interactions ($\alpha = 2$ in Eq. **15**) and a 50:50 bidisperse mixture of particles with diameter ratio 1:1.4. We also generate 2D packings with a uniform diameter distribution between 1 and 1.4 (data in *SI Text*).

Pressure–Shear Stress Exponent Equality

Here, we derive a key result by connecting the scaling of the pressure and shear stress to obtain the exponent relation

$$\delta_s = \delta_p + \frac{\psi}{2}. \quad [16]$$

The difference in scaling can be understood by considering the stress tensor, which is microscopically calculated using (53)

$$\sigma_{\alpha\beta} = -\frac{1}{V}\sum_k b^{(k)} \hat{r}_\alpha^{(k)} \hat{r}_\beta^{(k)}. \quad [17]$$

Here, α and β index spatial components, $\vec{r}^{(k)} = r^{(k)}\hat{r}^{(k)}$ is the vector connecting the centers of two particles along bond k, $\hat{r}^{(k)}$ is a unit vector, $f^{(k)}$ is the magnitude of the force on the bond, and $b^{(k)} = f^{(k)} r^{(k)}$. Therefore, the pressure (the typical diagonal components of $\sigma_{\alpha\beta}$) and the shear stress (the typical off-diagonal components) are set by the same residual forces. However, the off-diagonal components add incoherently, introducing an additional system size dependence in the shear stress.

The pressure of an individual system is

$$p = -\frac{1}{d}\mathrm{Tr}\sigma = \frac{1}{Vd}\sum_k b^{(k)} = \frac{N_b}{Vd}\langle b\rangle_k, \quad [18]$$

where $N_b = NZ/2$ is the number of bonds, and $\langle\cdot\rangle_k$ indicates an average over all bonds. We will indicate ensemble averages with a Λ subscript, and therefore, the ensemble average pressure is

$$\langle p\rangle_\Lambda = \frac{N_b}{Vd}\langle b\rangle_\Lambda. \quad [19]$$

Near the jamming transition, the pressure vanishes, but N_b/Vd is slowly varying. We may, therefore, regard N_b/Vd as constant, so that $\langle b\rangle_\Lambda$ obeys the same scaling as $\langle p\rangle_\Lambda$ as in Eq. **2**.

For an ensemble where the pressure is not held fixed, the fluctuations in p are described by

$$\delta p^2 \equiv \left\langle (p - \langle p\rangle_\Lambda)^2 \right\rangle_\Lambda. \quad [20]$$

Substituting in Eqs. **18** and **19**, Eq. **20** can be written as

$$\delta p^2 = \frac{N_b}{V^2 d^2}\sum_k \left[\left\langle b^{(0)} b^{(k)}\right\rangle_\Lambda - \langle b\rangle_\Lambda^2\right] \quad [21]$$

$$= \frac{N_b}{V^2 d^2}\left[\langle b^2\rangle_\Lambda - \langle b\rangle_\Lambda^2\right]$$

$$+ \frac{N_b}{V^2 d^2}\sum_{k\neq 0}\left(\left\langle b^{(0)} b^{(k)}\right\rangle_\Lambda - \langle b\rangle_\Lambda^2\right). \quad [22]$$

We now make two assumptions. First, one would expect that a microscopic quantity like $b^{(k)}$ should have a consistent scaling form, so that the distribution $P(b/\langle b\rangle_\Lambda)$ is independent of system size and ΔZ. This expectation is confirmed in Fig. S4, and it implies that the variance, $\langle b^2\rangle_\Lambda - \langle b\rangle_\Lambda^2$, is proportional to $\langle b\rangle_\Lambda^2$ and therefore scales like p^2. Similarly, the correlations $\langle b^{(0)} b^{(k)}\rangle_\Lambda$ with nearby bonds should scale like p^2. Second, we assume that the correlations between force moments $b^{(k)}$ decay rapidly with the distance between the bonds. This assumption is consistent with earlier assumptions made to derive the scaling of the shear modulus (21) and the widespread failure to find long-ranged force correlations in jammed systems. Thus, although there may be some very short-range correlations, this should not change the scaling of δp^2. Finally, because $N_b \sim V \sim N$, we see that

$$\delta p^2 \sim \frac{p^2}{N}. \quad [23]$$

Note that, because the pressure is proportional to $\langle b\rangle_\Lambda$, this result is what one would expect from the central limit theorem.

We now consider the residual shear stress, which is quantified by the deviatoric stress tensor

$$\tilde{\sigma}_{\alpha\beta} = \sigma_{\alpha\beta} - \frac{1}{d}\sigma_{\gamma\gamma}\delta_{\alpha\beta}. \quad [24]$$

However, $\langle\tilde{\sigma}_{\alpha\beta}\rangle_\Lambda = 0$ by symmetry, and therefore, we instead consider

$$s^2 \equiv \left\langle \tilde{\sigma}_{\alpha\beta}\tilde{\sigma}_{\alpha\beta}\right\rangle_\Lambda. \quad [25]$$

Note that Eq. **25** can also be written as $s^2 = \langle \mathrm{Tr}\left[\sigma - \frac{1}{d}\mathrm{Tr}\sigma\right]^2\rangle_\Lambda$. Substituting Eq. **17**, we have

$$s^2 = \frac{1}{V^2}\left\langle \sum_{kk'} b^{(k)} b^{(k')}\left[\cos^2(\theta_{kk'}) - \frac{1}{d}\right]\right\rangle_\Lambda, \quad [26]$$

where $\theta_{kk'}$ is the angle between bonds k and k'.

The sum can again be broken into two pieces:

$$s^2 = \frac{N_b}{V^2}\frac{d-1}{d}\langle b^2\rangle_\Lambda + \frac{N_b}{V^2}\sum_{k\neq 0}\left\langle b^{(0)} b^{(k)}\left[\cos^2(\theta_{0k}) - \frac{1}{d}\right]\right\rangle_\Lambda. \quad [27]$$

Note that, for an isotropic system, $\langle\cos^2(\theta_{0k}) - 1/d\rangle_\Lambda = 0$. If only short-range correlations exist, then the second term will again have the same scaling as the first term. More specifically, if we define the bond force moment correlation function

$$C_M(\vec{x}) = \left\langle \sum_{k\neq 0} b^{(0)} b^{(k)}\left(\hat{r}^{(0)}\hat{r}^{(k)} - \frac{1}{d}\right)\delta\left(\vec{x}^{(0,k)} - \vec{x}\right)\right\rangle_\Lambda, \quad [28]$$

where $\vec{x}^{(0,k)}$ is the vector between bond 0 and bond k, then

$$s^2 = \frac{N_b}{V^2}\left(\frac{d-1}{d}\langle b^2\rangle_\Lambda + \int C_M(\vec{x})\, d^d\vec{x}\right). \quad [29]$$

Thus, if there are no long-range correlations, then the final integral converges to a finite result as $N \to \infty$ that is proportional to $\langle b^2\rangle_\Lambda$. s^2 will then scale like $\langle b^2\rangle_\Lambda/N$, and because we have already seen that $\langle b^2\rangle_\Lambda \sim \langle b\rangle_\Lambda^2$, we have

$$s^2 \sim \frac{p^2}{N}. \quad [30]$$

We, therefore, expect $s^2 N/p^2 \sim \Delta Z^{2\delta_s - \psi - 2\delta_p}$ to be independent of ΔZ for sufficiently large N, implying our exponent relation

$\delta_s = \delta_p + \psi/2$ of Eq. **16**. In general, using Eq. **9** and Eq. **S12** (*SI Text*), we see that

$$\frac{s^2 N}{p^2} = f(N\Delta Z^{\Psi}). \quad [31]$$

Fig. S5 shows that this scaling form is obeyed (until analytic corrections become relevant at large ΔZ) (*SI Text*) and that s^2N/p^2 is constant over several decades of p as expected, affirming our analytical argument for the scaling relation of Eq. **16**. Finally, note that although the diagonal and off-diagonal components of the stress tensor scale differently with distance to the critical point, their fluctuations scale the same way.

ACKNOWLEDGMENTS. We thank Sid Nagel and Tom Lubensky for instructive discussions. This research was supported by US Department of Energy, Office of Basic Energy Sciences, Division of Materials Sciences and Engineering Award DE-FG02-05ER46199 (to C.P.G. and A.J.L.) and National Science Foundation Award DMR 1312160 (to J.P.S.). This work was partially supported by a University of Pennsylvania School of Arts and Sciences Dissertation Fellowship (C.P.G.) and a Simons Investigator Award from the Simons Foundation (to A.J.L.).

1. Liu AJ, Nagel SR (2010) The jamming transition and the marginally jammed solid. *Annu Rev Condens Matter Phys* 1(1):347–369.
2. O'Hern CS, Langer SA, Liu AJ, Nagel SR (2002) Random packings of frictionless particles. *Phys Rev Lett* 88(7):075507.
3. O'Hern CS, Silbert LE, Liu AJ, Nagel SR (2003) Jamming at zero temperature and zero applied stress: The epitome of disorder. *Phys Rev E Stat Nonlin Soft Matter Phys* 68(1 Pt 1):011306.
4. Liu AJ, Nagel SR (1998) Jamming is not just cool any more. *Nature* 396(6706):21–22.
5. Durian DJ (1995) Foam mechanics at the bubble scale. *Phys Rev Lett* 75(26):4780–4783.
6. Ellenbroek WG, Somfai E, van Hecke M, van Saarloos W (2006) Critical scaling in linear response of frictionless granular packings near jamming. *Phys Rev Lett* 97(25):258001.
7. Olsson P, Teitel S (2007) Critical scaling of shear viscosity at the jamming transition. *Phys Rev Lett* 99(17):178001.
8. Ellenbroek WG, van Hecke M, van Saarloos W (2009) Jammed frictionless disks: Connecting local and global response. *Phys Rev E Stat Nonlin Soft Matter Phys* 80(6 Pt 1):061307.
9. Dagois-Bohy S, Tighe BP, Simon J, Henkes S, van Hecke M (2012) Soft-sphere packings at finite pressure but unstable to shear. *Phys Rev Lett* 109(9):095703.
10. Goodrich CP, Liu AJ, Nagel SR (2012) Finite-size scaling at the jamming transition. *Phys Rev Lett* 109(9):095704.
11. Tighe BP (2012) Dynamic critical response in damped random spring networks. *Phys Rev Lett* 109(16):168303.
12. Goodrich CP, et al. (2014) Jamming in finite systems: Stability, anisotropy, fluctuations, and scaling. *Phys Rev E Stat Nonlin Soft Matter Phys* 90(2):022138.
13. van Deen MS, et al. (2014) Contact changes near jamming. *Phys Rev E Stat Nonlin Soft Matter Phys* 90(2):020202.
14. Silbert LE, Liu AJ, Nagel SR (2005) Vibrations and diverging length scales near the unjamming transition. *Phys Rev Lett* 95(9):098301.
15. Wyart M, Nagel SR, Witten TA (2005) Geometric origin of excess low-frequency vibrational modes in weakly connected amorphous solids. *EPL* 72:486.
16. During G, Lerner E, Wyart M (2012) Phonon gap and localization lengths in floppy materials. *Soft Matter* 9(1):146.
17. Goodrich CP, Ellenbroek WG, Liu AJ (2013) Stability of jammed packings. I: The rigidity length scale. *Soft Matter* 9(46):10993.
18. Schoenholz SS, Goodrich CP, Kogan O, Liu AJ, Nagel SR (2013) Stability of jammed packings. II: The transverse length scale. *Soft Matter* 9(46):11000.
19. Lerner E, DeGiuli E, Düring G, Wyart M (2014) Breakdown of continuum elasticity in amorphous solids. *Soft Matter* 10(28):5085–5092.
20. Vågberg D, Valdez-Balderas D, Moore MA, Olsson P, Teitel S (2011) Finite-size scaling at the jamming transition: Corrections to scaling and the correlation-length critical exponent. *Phys Rev E Stat Nonlin Soft Matter Phys* 83(3 Pt 1):030303.
21. Wyart M (2005) On the rigidity of amorphous solids. *Ann Phys (Paris)* 30(3):1–96.
22. Charbonneau P, Kurchan J, Parisi G, Urbani P, Zamponi F (2014) ncomms4725. *Nat Commun* 5:3725.
23. Widom B (1965) Equation of state in the neighborhood of the critical point. *J Chem Phys* 43(11):3898.
24. Myers CR, Sethna JP (1993) Collective dynamics in a model of sliding charge-density waves. I. Critical behavior. *Phys Rev B Condens Matter* 47(17):11171–11193.
25. Myers CR, Sethna JP (1993) Collective dynamics in a model of sliding charge-density waves. II. Finite-size effects. *Phys Rev B Condens Matter* 47(17):11194–11203.
26. Middleton AA, Fisher DS (1993) Critical behavior of charge-density waves below threshold: Numerical and scaling analysis. *Phys Rev B Condens Matter* 47(7):3530–3552.
27. Pázmándi F, Scalettar RT, Zimányi GT (1997) Revisiting the theory of finite size scaling in disordered systems: ν can be less than $2/d$. *Phys Rev Lett* 79:5130–5133.
28. Chaudhuri P, Berthier L, Sastry S (2010) Jamming transitions in amorphous packings of frictionless spheres occur over a continuous range of volume fractions. *Phys Rev Lett* 104(16):165701.
29. Markovic N, Christiansen C, Goldman AM (1998) Thickness magnetic field phase diagram at the superconductor-insulator transition in 2D. *Phys Rev Lett* 81(23):5217–5220.
30. Wyart M, Silbert LE, Nagel SR, Witten TA (2005) Effects of compression on the vibrational modes of marginally jammed solids. *Phys Rev E Stat Nonlin Soft Matter Phys* 72(5 Pt 1):051306.
31. Charbonneau P, Ikeda A, Parisi G, Zamponi F (2011) Glass transition and random close packing above three dimensions. *Phys Rev Lett* 107(18):185702.
32. Charbonneau P, Corwin EI, Parisi G, Zamponi F (2012) Universal microstructure and mechanical stability of jammed packings. *Phys Rev Lett* 109(20):205501.
33. Charbonneau P, Corwin EI, Parisi G, Zamponi F (2015) Jamming criticality revealed by removing localized buckling excitations. *Phys Rev Lett* 114(12):125504.
34. Yoshino H, Zamponi F (2014) Shear modulus of glasses: Results from the full replica-symmetry-breaking solution. *Phys Rev E Stat Nonlin Soft Matter Phys* 90(2):022302.
35. Binder K, Nauenberg M, Privman V, Young AP (1985) Finite-size tests of hyperscaling. *Phys Rev B Condens Matter* 31(3):1498–1502.
36. Wittmann M, Young AP (2014) Finite-size scaling above the upper critical dimension. *Phys Rev E Stat Nonlin Soft Matter Phys* 90(6):062137.
37. Wyart M, Liang H, Kabla A, Mahadevan L (2008) Elasticity of floppy and stiff random networks. *Phys Rev Lett* 101(21):215501.
38. Nakayama D, Yoshina H, Zamponi F (2015) Protocol-dependent shear modulus of amorphous solids. arXiv:1512.06544.
39. Boschan J, Vågberg D, Somfai E, Tighe BP (2016) Beyond linear elasticity: Jammed solids at finite shear strain and rate. *Soft Matter* 12(24):5450–5460.
40. Bi D, Zhang J, Chakraborty B, Behringer RP (2011) Jamming by shear. *Nature* 480(7377):355–358.
41. Wyart M (2011) Elasticity of soft particles and colloids near random close packing. *Microgels: Synthesis, Properties and Applications*, eds Fernandez A, Mattsson J, Wyss H, Weitz D (Wiley, Weinheim, Germany), pp 195–206.
42. Tighe BP (2011) Relaxations and rheology near jamming. *Phys Rev Lett* 107(15):158303.
43. DeGiuli E, Düring G, Lerner E, Wyart M (2015) Unified theory of inertial granular flows and non-Brownian suspensions. *Phys Rev E Stat Nonlin Soft Matter Phys* 91(6):062206.
44. Fisher DS (1986) Scaling and critical slowing down in random-field Ising systems. *Phys Rev Lett* 56(5):416–419.
45. Ikeda A, Berthier L, Biroli G (2013) Dynamic criticality at the jamming transition. *J Chem Phys* 138(12):12A507.
46. Wang L, Xu N (2013) Critical scaling in thermal systems near the zero-temperature jamming transition. *Soft Matter* 9(8):2475.
47. Lerner E, Düring G, Wyart M (2012) A unified framework for non-brownian suspension flows and soft amorphous solids. *Proc Natl Acad Sci USA* 109(13):4798–4803.
48. Lerner E, Düring G, Wyart M (2012) Toward a microscopic description of flow near the jamming threshold. *EPL* 99(5):58003.
49. Lin J, Lerner E, Rosso A, Wyart M (2014) Scaling description of the yielding transition in soft amorphous solids at zero temperature. *Proc Natl Acad Sci USA* 111(40):14382–14387.
50. Ulrich S, Upadhyaya N, van Opheusden B, Vitelli V (2013) *Shear Shocks in Fragile Networks. Proc Natl Acad Sci USA* 110(52):20929–20934.
51. Vitelli V, Xu N, Wyart M, Liu AJ, Nagel SR (2010) Heat transport in model jammed solids. *Phys Rev E Stat Nonlin Soft Matter Phys* 81(2 Pt 1):021301.
52. Bitzek E, Koskinen P, Gähler F, Moseler M, Gumbsch P (2006) Structural relaxation made simple. *Phys Rev Lett* 97(17):170201.
53. Hansen J, McDonald I (2006) *Theory of Simple Liquids* (Elsevier Science, Amsterdam).

Supporting Information

Goodrich et al. 10.1073/pnas.1601858113

SI Text

1. Changing Ensembles and Integrating over the ΔZ Distribution. Eqs. **1–5** can be easily adapted to the fixed $p\varepsilon N$ ensemble by inverting Eq. **2**,

$$\frac{\Delta\phi}{\Delta Z^{\beta_\phi}} = \Phi\left(\frac{p}{\Delta Z^{\delta_p}}, \frac{\varepsilon}{\Delta Z^{\beta_\varepsilon}}, N\Delta Z^{\Psi}\right), \quad [S1]$$

and inserting this into Eqs. **1** and **3–5**. The other scaling functions can then be written as functions of the scaled pressure, shear strain, and system size, taking the forms

$$E = \Delta Z^{\zeta}\mathcal{E}\left(\frac{p}{\Delta Z^{\delta_p}}, \frac{\varepsilon}{\Delta Z^{\beta_\varepsilon}}, N\Delta Z^{\Psi}\right), \quad [S2]$$

$$s = \Delta Z^{\delta_s}\mathcal{S}\left(\frac{p}{\Delta Z^{\delta_p}}, \frac{\varepsilon}{\Delta Z^{\beta_\varepsilon}}, N\Delta Z^{\Psi}\right), \quad [S3]$$

$$B = \Delta Z^{\gamma_B}\mathcal{B}\left(\frac{p}{\Delta Z^{\delta_p}}, \frac{\varepsilon}{\Delta Z^{\beta_\varepsilon}}, N\Delta Z^{\Psi}\right), \quad [S4]$$

and

$$G = \Delta Z^{\gamma_G}\mathcal{G}\left(\frac{p}{\Delta Z^{\delta_p}}, \frac{\varepsilon}{\Delta Z^{\beta_\varepsilon}}, N\Delta Z^{\Psi}\right). \quad [S5]$$

Note that the scaling functions in Eqs. **S2–S5** are different from those appearing in Eqs. **1–5**. It is straightforward to adjust the theory to other ensembles, such as the fixed $\Delta\phi\, sN$ ensemble of the original jamming phase diagram (4) or the fixed psN ensemble of ref. 9.

Recall that ΔZ is not externally controlled but instead, is measured for packings at a given p, ε, and N, forming the probability distribution $R(\Delta Z|p,\varepsilon,N)$. The scaling hypothesis implies that the probability distribution $R(\Delta Z|p,\varepsilon,N)$ for ΔZ should take the form

$$R(\Delta Z|p,\varepsilon,N) = p^{-\frac{1}{\delta_p}}\mathcal{R}\left(\frac{\Delta Z}{p^{\frac{1}{\delta_p}}}, \frac{\varepsilon}{p^{\frac{\beta_\varepsilon}{\delta_p}}}, Np^{\frac{\Psi}{\delta_p}}\right), \quad [S6]$$

where we have taken combinations of the natural scaling variables so that only the first variable depends on ΔZ. The prefactor p^{-1/δ_p} normalizes the distribution. Changing variables to $W = \Delta Z/p^{1/\delta_p}$, $X = \varepsilon/p^{\beta_\varepsilon/\delta_p}$, and $Y = Np^{\Psi/\delta_p}$, we can integrate over the distribution to obtain the average of W:

$$\langle W\rangle = \int \mathcal{R}(W,X,Y)WdW. \quad [S7]$$

Defining $\mathcal{Z}(X,Y) \equiv Y^{1/\Psi}\int \mathcal{R}(W,X,Y)WdW$, we can write this as

$$N^{\frac{1}{\Psi}}\langle\Delta Z\rangle = \mathcal{Z}\left(\frac{\varepsilon}{p^{\frac{\beta_\varepsilon}{\delta_p}}}, Np^{\frac{\Psi}{\delta_p}}\right). \quad [S8]$$

Dropping the $\langle.\rangle$ notation and inverting $\mathcal{Z}$ with respect to the second argument, we see that

$$p = N^{-\frac{\delta_p}{\Psi}}F_1\left(\frac{\varepsilon}{\Delta Z^{\beta_\varepsilon}}, N\Delta Z^{\Psi}\right). \quad [S9]$$

Dividing by ΔZ^{δ_p}, we can write

$$\frac{p}{\Delta Z^{\delta_p}} = \frac{N^{-\frac{\delta_p}{\Psi}}F_1\left(\frac{\varepsilon}{\Delta Z^{\beta_\varepsilon}}, N\Delta Z^{\Psi}\right)}{\Delta Z^{\delta_p}} \quad [S10]$$

$$= (N\Delta Z^{\Psi})^{-\frac{\delta_p}{\Psi}}F_1\left(\frac{\varepsilon}{\Delta Z^{\beta_\varepsilon}}, N\Delta Z^{\Psi}\right) \quad [S11]$$

$$= F_2\left(\frac{\varepsilon}{\Delta Z^{\beta_\varepsilon}}, N\Delta Z^{\Psi}\right). \quad [S12]$$

Note that the scaling function F_2 could depend slightly on the details of the numerical protocol used to create the systems. Because of this interdependency between the scaling variables, we see that the scaling functions in Eqs. **S1–S5** can be written in terms of just two variables, $\varepsilon/\Delta Z^{\beta_\varepsilon}$ and $N\Delta Z^{\Psi}$. Furthermore, for unsheared packings, $\varepsilon = 0$ by our definition, and therefore, in that case, the number of variables in the scaling functions is reduced to only one, $N\Delta Z^{\Psi}$. Therefore, our theory predicts

$$E = \Delta Z^{\zeta}\mathcal{E}(N\Delta Z^{\Psi}), \quad [S13]$$

$$\Delta\phi = \Delta Z^{\beta_\phi}\Phi(N\Delta Z^{\Psi}), \quad [S14]$$

$$s = \Delta Z^{\delta_s}\mathcal{S}(N\Delta Z^{\Psi}), \quad [S15]$$

$$B = \Delta Z^{\gamma_B}\mathcal{B}(N\Delta Z^{\Psi}), \quad [S16]$$

$$G = \Delta Z^{\gamma_G}\mathcal{G}(N\Delta Z^{\Psi}), \quad [S17]$$

and as well as

$$N^{\frac{1}{\Psi}}\Delta Z = \mathcal{Z}\left(Np^{\frac{\Psi}{\delta_p}}\right). \quad [S18]$$

2. Corrections to Scaling. Here, we examine the scaling collapses at the upper critical dimension, $d_u = 2$, where we expect singular corrections to scaling to be important. We also include analytic corrections to scaling at large ΔZ in $d = 3$. Both types of corrections to scaling are expected for critical phase transitions and in no way contradict the ideas presented in the text. We begin by showing numerical data for the energy, pressure, shear stress, bulk modulus, and shear modulus, scaled according to our theory, for systems in the fixed $p\varepsilon N$ ensemble in both two (Fig. S1) and three dimensions (Fig. S2). Note that, compared with Figs. 1 and 2, here we extended the data to larger ΔZ.

The 2D data in Fig. S1 show clear systematic deviations from scaling in the energy, pressure, shear stress, and to a lesser extent, shear modulus. Such deviations from scaling are expected at the upper critical dimension of a phase transition and are not observed in three dimensions (Fig. S2). Also, note that (except for B), these deviations are relatively small compared with the singular behavior, which is scaled out in each plot (see figure 6 in ref. 12). Therefore, for an extreme example, the energy collapse is good only to a factor of about four, but the energies span a range of 10^{14}, because ΔZ varies by at least 10^4. Although we do not have a theoretical prediction for the form that such corrections should take, it has been shown that such data can be collapsed by introducing logarithmic corrections (12, 13). However,

we find that including small corrections to the scaling exponents works equally well (Fig. S1, *Inset* in row 2).

A scaling ansatz describes only the leading order behavior near a critical point. Subdominant corrections to scaling can and often do exist. As one might, therefore, expect, the scaling collapse in Figs. 1 and 2 as well as the collapse of B, G, etc. break down if the data are extended to larger ΔZ. Fig. S2 clearly shows this for 3D data. Far from the critical point ($\Delta Z \sim 1$), one expects analytic corrections to scaling, reflecting the noncritical dependence of energy and other properties on external parameters. We find the deviations in our 3D data can be described all the way to $\Delta Z \approx 0.5$ by incorporating an overall multiplicative analytic correction to scaling. Expanding the analytic correction to E about the critical point, our ansatz can be written as

$$E = \Delta Z^{\zeta} \mathcal{E}_0 \left(\frac{\Delta\phi}{\Delta Z^{\beta_\phi}}, \frac{\varepsilon}{\Delta Z^{\beta_\varepsilon}}, N\Delta Z^{\psi} \right) (1 + e_1 \Delta Z + \ldots). \qquad \textbf{[S19]}$$

Eq. **S19** suggests that the energy should collapse by dividing $E\Delta Z^{-\zeta}$ by $1 + e_1\Delta Z$ for some appropriately chosen e_1, which is confirmed in Fig. S3, *Upper*, where we have set $e_1 = -0.13$. Analytic corrections are not restricted to the scaling of the energy, and it is clear from our theory how the higher-order terms in Eq. **S19** should propagate to the scaling of other quantities. For example, including linear corrections to the scaling of the bulk modulus gives

$$B = \Delta Z^{\gamma_B} \mathcal{B}(N\Delta Z^{\psi})(1 + b_1 \Delta Z + \ldots), \qquad \textbf{[S20]}$$

suggesting that we should get data collapse by dividing $B\Delta Z^{-\gamma_B}$ by $1 + b_1\Delta Z$, which is confirmed by Fig. S3, *Lower* (recall that $\gamma_B = 0$), where $b_1 = 0.5$. Finally, note that if the corrections to scaling in Eqs. **S19** and **S20** were written in terms of the pressure p or the excess packing fraction $\Delta\phi$, the leading correction would be proportional to $\sqrt{p}$ or $\sqrt{\Delta\phi}$. The fact that the corrections are linear in ΔZ suggest that ΔZ is, indeed, a natural control variable for the theory, although it technically depends on p or $\Delta\phi$, depending on ensemble.

3. Review of Theoretical Arguments for Scaling Exponents. In the text, we used known numerical results to extract the exponents δ_p, γ_B, γ_G, and ψ, from which we obtained the other exponents from Eq. **6**. Because we then derived the scaling relation $\gamma_G = \gamma_B + \psi$, we actually only needed to extract δ_p, γ_B, and ψ to fully determine all scaling exponents. Here, we provide a brief review of some previous theoretical arguments for δ_p, γ_B and ψ, so that the full theory rests on theoretical rather than numerical grounds. We emphasize that there are multiple ways of understanding these relations, and therefore, the arguments given here are not unique.

In ref. 21, Wyart showed that the scaling of the excess contact number with the pressure can be understood as follows. The frequency of the lowest vibrational mode (excluding phonons) can be written as $\omega_0^2 = A_1\Delta Z^2 - A_2 p$, where A_1 and A_2 are positive constants. The first term, $A_1\Delta Z^2$, comes from a variational argument (15) for the spectrum of a sphere packing in the absence of stresses, whereas the second term, $-A_2 p$, results from reintroducing the prestress on each particle–particle contact. Because $\omega_0^2 \geq 0$ for a stable packing, we obtain the bound $\Delta Z \geq C_0 p^{1/2}$. Wyart (21) argues that this becomes an equality for jammed sphere packings, because rearrangements only result from instabilities and have the effect of making the system only marginally stable. Therefore, $p \sim \Delta Z^2$, and $\delta_p = 2$.

From this result, Goodrich et al. (10) showed that $\psi = 1$ follows by considering finite-size systems very near the jamming transition. Because a jammed system must always have at least one contact in excess of the isostatic number of contacts to support a pressure, the contact number Z is bounded by $Z - Z_{\text{iso}} \geq 2/N$, where $Z_{\text{iso}} \equiv 2d - 2d/N$. Thus, one would expect a cross-over in the scaling from $Z - Z_{\text{iso}} \sim p^{1/2}$ at high pressure to $Z - Z_{\text{iso}} \sim 1/N$ at low pressure. Therefore, if scaling collapse exists, it must be of the form $(Z - Z_{\text{iso}})N = \tilde{\mathcal{Z}}(p^{1/2}N)$, where $\tilde{\mathcal{Z}}(x) \to 2$ as $x \to 0^+$. Recall that, here, we have defined $\Delta Z \equiv Z - Z_{\text{iso}} - 2/N$, and therefore, we have $N\Delta Z = \mathcal{Z}(p^{1/2}N)$, where $\mathcal{Z}(x) = \tilde{\mathcal{Z}}(x) - 2$. Comparing this form with Eq. **12** and using $\delta_p = 2$, we see that $\psi = 1$.

Finally, Wyart (21) understood the scaling of the bulk modulus by writing the energy of a deformation as a sum of the projection of the deformation on the various states of self-stress. For packings of purely repulsive spheres, there is a state of self-stress with only positive components that projects entirely onto hydrostatic compression and dominates the response near the jamming transition. Because the response does not depend (to leading order) on the total number of states of self-stress and thus on ΔZ, we have $B \sim \Delta Z^0$. Therefore, we see that $\gamma_B = 0$.

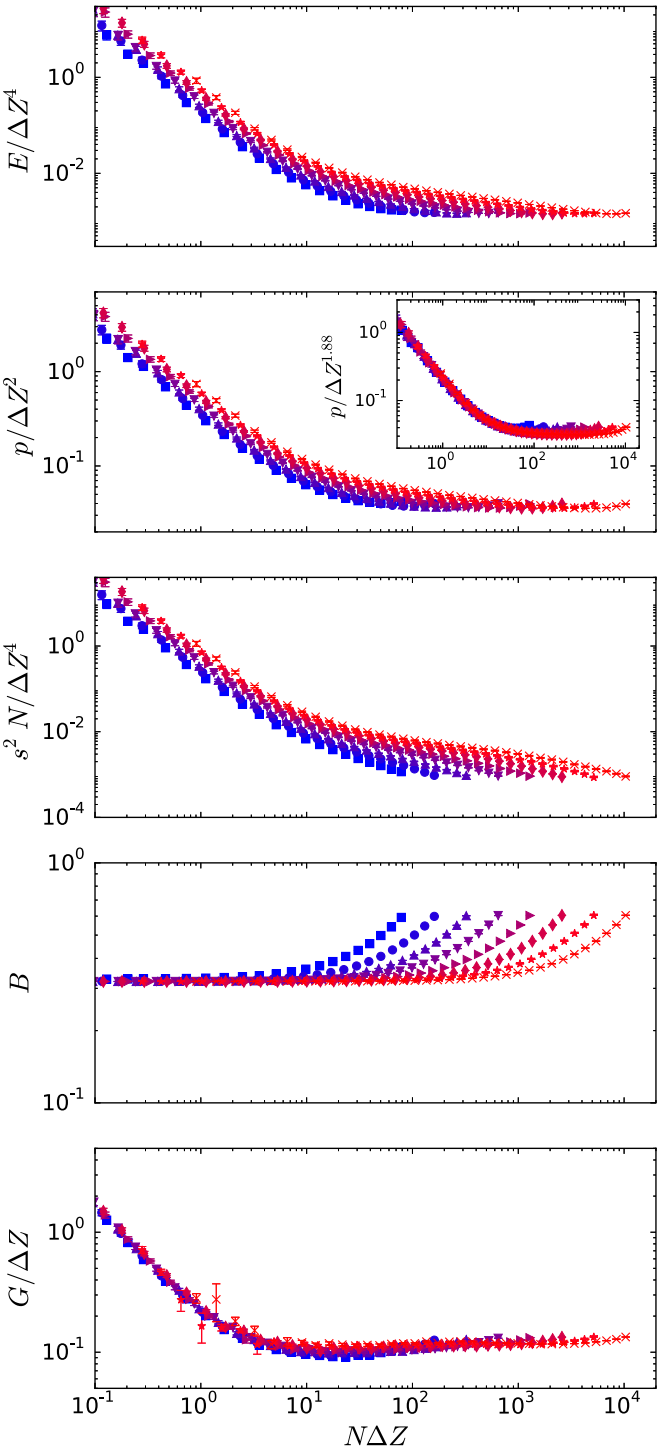

Fig. S1. Scaling in two dimensions. In rows 1–5, the energy, pressure, shear stress, bulk modulus, and shear modulus, respectively, are all scaled according to our theory. Small singular corrections to scaling as well as analytic corrections at large ΔZ are observed. In 2D, we include $N = 8,192$ systems (red crosses); the rest of the symbols and colors have the same meaning as in Fig. 1.

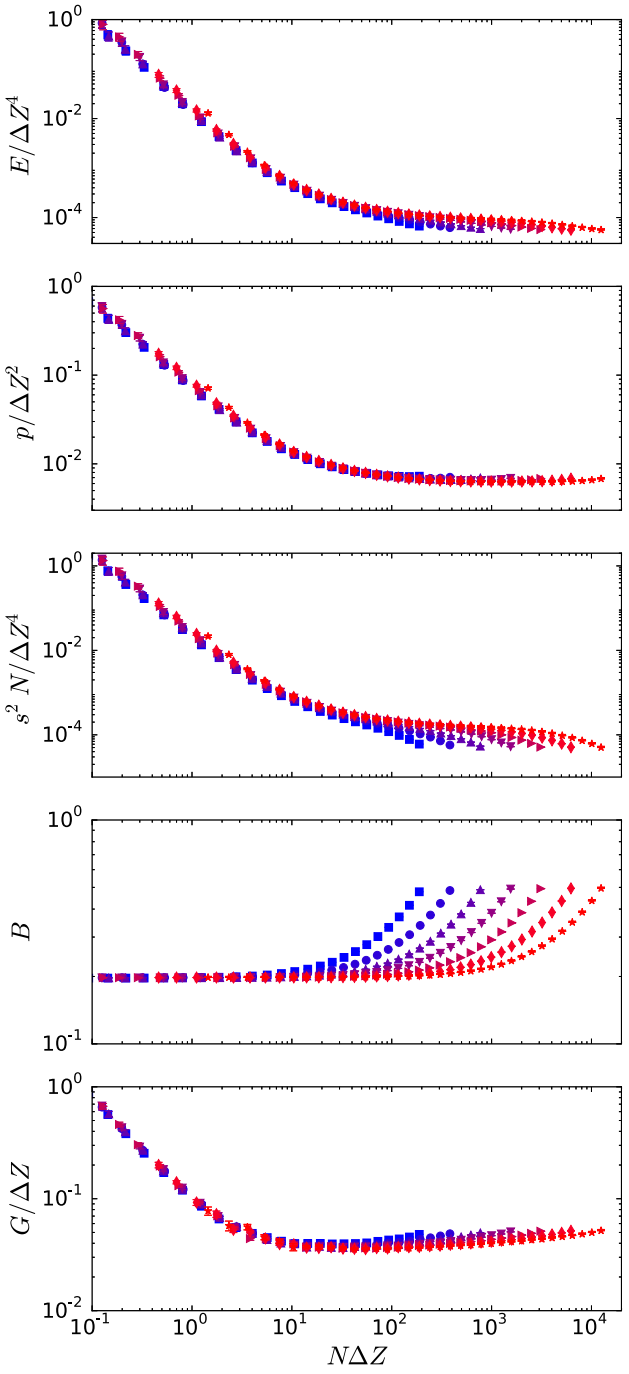

Fig. S2. Scaling in three dimensions. In rows 1–5, the energy, pressure, shear stress, bulk modulus, and shear modulus, respectively, are all scaled according to our theory. Data are extended to higher ΔZ than what is shown in Figs. 1 and 2, and analytic corrections to scaling are observed in this region. Symbols and colors have the same meaning as in Fig. 1.

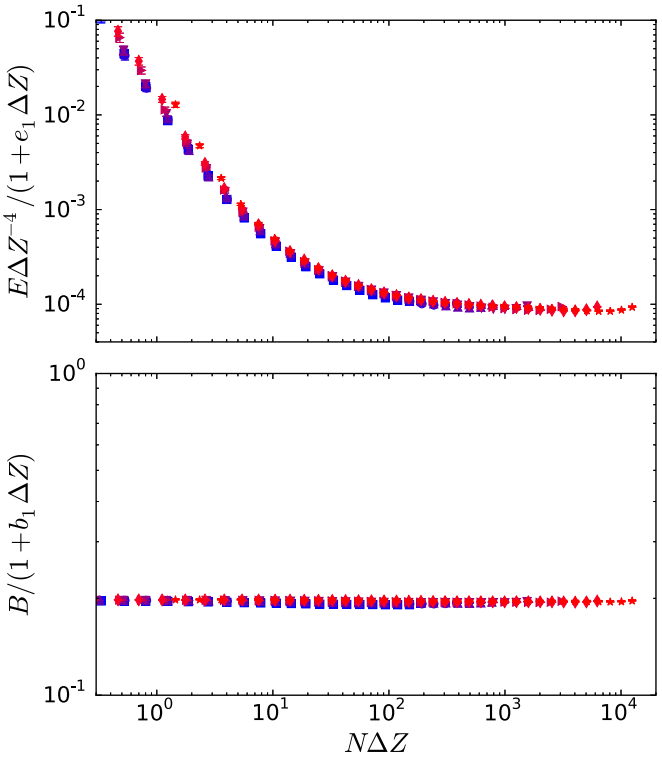

Fig. S3. Analytic corrections to scaling at large ΔZ for 3D data. (*Upper*) $E\Delta Z^{-4}/(1+e_1\Delta Z)$, where $e_1=-0.13$. (*Lower*) $B/(1+b_1\Delta Z)$, where $b_1=0.5$. Symbols and colors have the same meaning as in Fig. 1. For comparison, the scale on the *y* axis corresponds to that in Fig. S2.

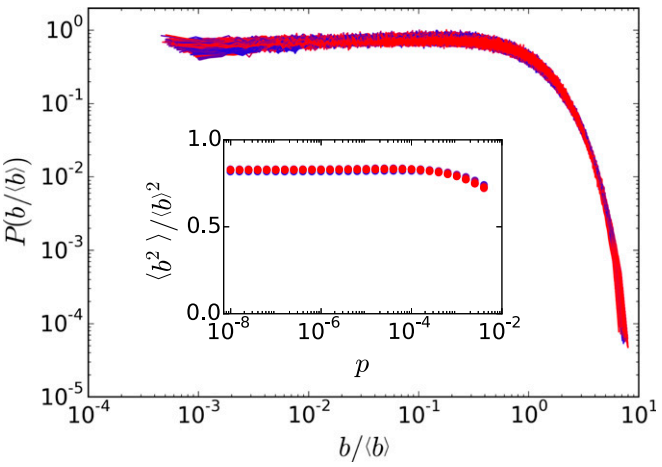

Fig. S4. Collapse of the distribution $P(b/\langle b\rangle)$ for different system sizes and ΔZ. (*Inset*) $\langle b^2\rangle \sim \langle b\rangle^2$ over many decades in pressure (or equivalently, ΔZ). Symbols and colors have the same meaning as in Fig. 1.

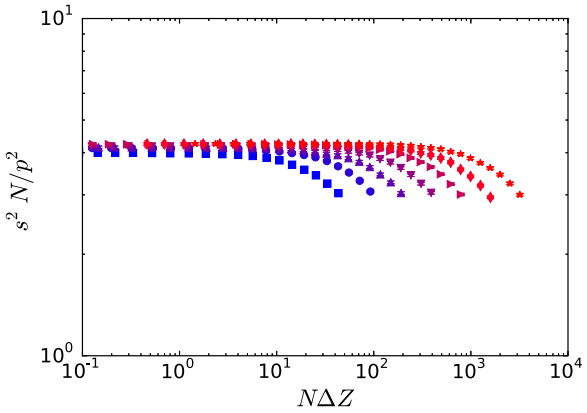

Fig. S5. Verification of the pressure–shear stress exponent relation. s^2N/p^2 is constant over several decades in $N\Delta Z$ until ΔZ is large enough so that analytic corrections to scaling become important (*SI Text*). Symbols and colors have the same meaning as in Fig. 1.